

AN INVESTIGATION OF PRESSURE DRAG IN TRANSONIC
FLOW BY THE METHOD OF HYDRAULIC ANALOGY

127

A THESIS


Presented to
the Faculty of the Graduate Division
Georgia Institute of Technology

In Partial Fulfillment
of the Requirements for the Degree
Master of Science in Aeronautical Engineering

by
Robert Thomas Stancil

July, 1954

"In presenting the dissertation as a partial fulfillment of the requirements for an advanced degree from the Georgia Institute of Technology, I agree that the Library of the Institution shall make it available for inspection and circulation in accordance with its regulations governing materials of this type. I agree that permission to copy from, or to publish from, this dissertation may be granted by the professor under whose direction it was written, or such copying or publication is solely for scholarly purposes and does not involve potential financial gain. It is understood that any copying from, or publication of, this dissertation which involves potential financial gain will not be allowed without written permission.



AN INVESTIGATION OF PRESSURE DRAG IN TRANSONIC
FLOW BY THE METHOD OF HYDRAULIC ANALOGY

Approved:

[Handwritten signature]

Date Approved by Chairman: 30 July 1954

ACKNOWLEDGEMENTS

The author is particularly indebted to Dr. R. G. Fleddermann for the suggestion of the topic and his invaluable assistance in the completion of the problem. Thanks must also be extended to Professor M. R. Carstens and Professor H. W. S. LaVier for their suggestions and constructive criticisms.

TABLE OF CONTENTS

	Page
ACKNOWLEDGMENTS.....	ii
LIST OF SYMBOLS.....	iv
LIST OF ILLUSTRATIONS.....	vi
SUMMARY.....	vii
 Chapter	
1. INTRODUCTION.....	1
II. THEORY.....	3
III. EQUIPMENT.....	17
IV. PROCEDURE.....	20
V. DISCUSSION OF RESULTS.....	21
VI. CONCLUSIONS.....	25
VII. RECOMMENDATIONS.....	26
APPENDIX.....	27
BIBLIOGRAPHY.....	33

LIST OF SYMBOLS

- a = Speed of sound in gas
 a^* = Speed of sound in gas at the point where the velocity equals the speed of sound
 C_p = Local pressure coefficient
 C_d = Section drag coefficient
 c_p = Specific heat of gas at constant pressure
 c_v = Specific heat of gas at constant volume
 γ = Adiabatic gas constant, ratio of c_p to c_v
 d = Water depth
 δ = Wedge angle in radians
 g = Acceleration due to gravity
 h = Enthalpy of gas
 ∞ = Infinity
 M = Mach number
 p = Pressure of gas
 ρ = Density of gas
 T = Absolute temperature of gas
 V = Velocity of flow
 ϕ = Velocity potential in two-dimensional flow
 θ = Angle of inclination of the velocity vector
 $\theta_0 = \delta/2$
 x, y = Rectangular coordinates in the flow plane
 u, v = Components of flow velocity in x and y directions, respectively
 $u = u - a^*$

LIST OF SYMBOLS (CON'T)

Subscripts

No subscript = Local value of variable

o = Value at stagnation

s = Value in undisturbed stream

max = Maximum value of variable

x = Partial derivative with respect to x

$$\text{e.g. } \phi_x = \frac{\partial \phi}{\partial x}, \quad \phi_{xx} = \frac{\partial^2 \phi}{\partial x^2}$$

y = Partial derivative with respect to y

LIST OF ILLUSTRATIONS

Figure	Page
1. Pressure Drag Coefficient for a 15° Wedge at Zero Angle of Attack.....	23
2. General View of the Water Channel.....	28
3. Transonic Flow Around a Wedge Airfoil....	29
4. Wedge Airfoil Model.....	30
5. Meniscus Effect.....	31
6. Pressure Distributions Over a 15° Wedge at Zero Angle of Attack.....	32

SUMMARY

This thesis was undertaken in an effort to compare the pressure drag coefficients in the transonic range of velocities obtained by the hydraulic analogy with the values predicted by theory and substantiated by shock tube experiments. A 15° wedge airfoil was tested at zero angle of attack at transonic speeds in the Georgia Institute of Technology twenty foot by four foot water channel. The water depth distributions along the side of the model were obtained by the probe method. By application of the hydraulic analogy, pressure distributions were found and from these pressure distributions the drag coefficients were calculated.

According to the theory the stagnation point at the nose of the airfoil causes a large pressure increase at that point, and the pressure falls off gradually toward the rear of the airfoil. In this investigation all tests were made either with no bow wave (subsonic flow) or with a detached bow wave. Thus in all cases a stagnation point is present at the nose. The results of this investigation did not show the expected high pressures over the front of the model, particularly at the higher speeds. It was concluded that the effect of vertical accelerations which are neglected in the theory of the hydraulic analogy was responsible for the fact that the water depths did not reach the expected height. Thus the hydraulic analogy for Mach numbers in the transonic range or greater does not give accurate results in the neighborhood of a stagnation point.

The drag coefficients calculated by means of the hydraulic analogy follow the general trend predicted by the theory but because of the error

in the pressure distribution, which was discussed above, the drag coefficients obtained from the hydraulic analogy do not compare accurately with the theoretical and shock tube results although the trend of the data is the same as for the other results.

CHAPTER I

INTRODUCTION

The problem of flow around bodies at transonic velocities has been troublesome to deal with, either theoretically or experimentally. An exact theoretical solution has not yet been found because: first, the partial differential equation is of the mixed type and is nonlinear; second, the locations of the boundaries of the transonic zone are not known at the start but must be determined as part of the solution; and third, the flow in the transonic zone for $M_S > 1$, having passed through the curved bow wave, is necessarily rotational. Experimental solutions have been difficult because of wind tunnel choking at speeds close to the speed of sound.

Theoretical investigations of the flow around a symmetrical wedge airfoil at transonic velocities by means of transonic perturbations by Cole¹, Guderly and Yoshihara², and Vincenti and Wagoner³, have provided an approximate theory which bridges the gap between the theory for pure subsonic flow and that for pure supersonic flow. Also experimental knowledge has recently been increased by a shock tube study of the transonic flow over symmetrical wedges by Griffith⁴. The experimental data of Griffith agrees with the approximate theory. The main result of both theory and experiment appears to be the invariance of local Mach number.

The fact that choking of the flow can easily be eliminated makes the hydraulic analogy applicable to transonic flow. This practical

consideration and the fact that it assumes a negligible effect of viscosity and rotationality immediately suggest the possibility of using it for comparison with the approximate theory which also neglects viscosity and rotationality.

CHAPTER II

THEORY

Hydraulic Analogy

Theoretical work on the analogy between flow of water with a free surface and compressible gas flow was first presented by Riabouchinsky⁵ in 1932. Since that time, further extensions of this theory and practical applications have been made by such leaders in the field as Ernst Preiswerk⁶, Binnie and Hooker⁷ in England, the National Advisory Committee for Aeronautics⁸, and North American Aviation Incorporated⁹, and Massachusetts Institute of Technology.¹⁰ Preiswerk's proof and explanations of the application of gas dynamics methods to the flow of water with a free surface are probably the foremost in the field. He conclusively proved the validity of the hydraulic analogy as it stands today.

North American Aviation and the National Advisory Committee for Aeronautics were leaders in experimental applications of the hydraulic analogy. Their work indicated that with the proper equipment and methods accurate quantitative as well as qualitative results could be expected from the water channel experiments.

Some of the advantages obtained through application of the hydraulic analogy and use of the water channel may be summarized as follows:

- (1) The relative cost is low compared with the wind tunnel or flight tests.
- (2) Visual observations for the purposes of research or

instruction of such phenomena as shock wave formation, vortices, turbulence, and flow patterns are possible.

- (3) High supersonic Mach numbers are obtained at model speeds of a few feet per minute.
- (4) Any Mach number can be achieved by a simple speed setting while a relatively complicated nozzle change is required in wind tunnel work.
- (5) Since choking can be easily eliminated, transonic observations are just as simple as for subsonic and supersonic speeds in the movable model type of water channel.

The present investigation is largely concerned with (5) above, since the tests were conducted at Mach numbers close to unity. Supersonic and subsonic test results have proved the water channel experimental values to be reliable. By virtue of this fact it was expected that the transonic water channel results would also be reliable.

The theory of the hydraulic analogy as presented by Ernst Preiswerk⁶ will be reviewed here.

This theory of the analogy between water flow with a free surface and the two-dimensional compressible gas flow depends on the following assumptions:

- (1) The flow is irrotational.
- (2) The vertical acceleration of the water is negligible compared with the acceleration due to gravity so that pressures in the fluid depend only on the height of the free surface above the point in question.
- (3) There are no viscous losses, thus excluding the conversion

of energy into heat or internal energy.

The energy equations for water and for gas give the relations shown below in terms of velocity.

For water this equation gives

$$V^2 = 2 g (d_o - d)$$

$$V_{\max} = \sqrt{2 g d_o}$$

and for gas

$$V^2 = 2 g c_p (T_o - T)$$

$$V_{\max} = \sqrt{2 g c_p T_o}$$

It can be seen that V/V_{\max} for water and air are equal if

$$\frac{T_o - T}{T_o} = \frac{d_o - d}{d_o}$$

or, if

$$\frac{d}{d_o} = \frac{T}{T_o} \tag{1}$$

This comparison of the depth ratio, d/d_o , to the gas temperature ratio, T/T_o , in the consideration of velocity is the first step in the proof of the analogy.

The equations of continuity are now compared. For steady two-dimensional gas flow, this equation is

$$\frac{\partial (u \rho)}{\partial x} + \frac{\partial (v \rho)}{\partial y} = 0$$

and for water

$$\frac{\partial (u d)}{\partial x} + \frac{\partial (v d)}{\partial y} = 0 \quad .$$

from these equations, a further step in the analogy is evolved as

$$\frac{d}{d_0} = \frac{p}{p_0} \quad . \quad (2)$$

By comparing equation (1) and (2), it is seen that the analogy holds only if the following equation is satisfied by the gas in question.

$$\frac{T}{T_0} = \frac{p}{p_0} \quad (3)$$

However, the temperature and pressure of the gas must also conform to the principles of the adiabatic relation (assumption 3):

$$\left(\frac{T}{T_0}\right)^{\frac{1}{\gamma-1}} = \frac{p}{p_0} \quad . \quad (4)$$

An inspection of equations (3) and (4) reveals that they are satisfied simultaneously only if $\gamma = 2$.

Thus, the flow of water is analogous to the flow of a gas having $\gamma = 2$. Since γ for air is 1.4, this appears to be rather loose comparison. However, many characteristics of gas flow do not depend strongly on γ . The significance of this statement will be further illustrated.

Consider now the adiabatic relation and the preceding numbered equations,

$$\frac{p}{p_0} = \left(\frac{p}{p_0}\right)^{\gamma} = \left(\frac{p}{p_0}\right)^2$$

or

$$\frac{p}{p_0} = \left(\frac{d}{d_0}\right)^2 \quad . \quad (5)$$

The differential equation of the velocity potential for water is as follows:

$$\phi_{xx} \left(1 - \frac{\phi_x^2}{gd}\right) + \phi_{yy} \left(1 - \frac{\phi_y^2}{gd}\right) - 2\phi_{xy} \frac{\phi_x \phi_y}{gd} = 0 \quad (6)$$

and the corresponding equation for gas is

$$\phi_{xx} \left(1 - \frac{\phi_x^2}{a^2}\right) + \phi_{yy} \left(1 - \frac{\phi_y^2}{a^2}\right) - 2\phi_{xy} \frac{\phi_x \phi_y}{a^2} = 0 \quad . \quad (7)$$

Equations (6) and (7) are identical if

$$\frac{gd}{2gd_0} = \frac{a^2}{2gh_0} \quad .$$

From this relation it is seen that \sqrt{gd} corresponds to the pressure propagation velocity or velocity of sound, a , in gas flow. The expression \sqrt{gd} is the basis wave propagation velocity in shallow water with a free surface as proved by Leigh Page.¹¹

In water flowing at speeds above \sqrt{gd} the velocity of the flow may rapidly decrease for short distances and the depth may increase. An unsteady motion of this type is called a hydraulic jump, and corresponds to a shock wave in a gas.

This completes the analogy which is summarized in the following table of corresponding quantities and characteristics.

Two-Dimensional Compressible Gas Flow, $\gamma = 2$	Analogous Liquid Flow
Temperature ratio, T/T_0	Water-depth ratio, d/d_0
Density ratio, ρ/ρ_0	Water-depth ratio, d/d_0
Pressure ratio, p/p_0	Square of water depth ratio, $(d/d_0)^2$
Velocity of sound, $a = \sqrt{\frac{\gamma p}{\rho}}$	Wave velocity, \sqrt{gd}
Mach number, V/a	Froude number, V/\sqrt{gd}
Shock Wave	Hydraulic jump

The application of the analogy as it will be used in this investigation will be listed in the paragraphs which follow.

The Mach number of the free stream will be calculated as

$$M_s = F_s = \frac{V_s}{\sqrt{gd}} \quad (8)$$

which by virtue of the hydraulic analogy will be referred to as Mach number hereafter in this discussion.

The standard equation for the pressure coefficient at any point on an airfoil as defined as

$$C_p = \frac{p - p_s}{\frac{1}{2} \rho_s V_s^2} \quad (9)$$

Since

$$\begin{aligned} \frac{1}{2} \rho_s V_s^2 &= \frac{1}{2} \rho_s a_s^2 M_s^2 \\ &= \frac{1}{2} \rho_s \left(\frac{\gamma p_s}{\rho_s} \right) M_s^2 \\ &= \frac{\gamma}{2} p_s M_s^2 \end{aligned}$$

equation (9) simplifies to

$$C_p = \frac{2}{\gamma M_s^2} \left[\frac{p}{p_s} - 1 \right] .$$

From equation (5)

$$\frac{p}{p_s} = \left(\frac{d}{d_s} \right)^2 .$$

Therefore, in the present case ($\gamma=2.0$), equation (9) becomes

$$C_p = \frac{1}{M_s^2} \left[\left(\frac{d}{d_s} \right)^2 - 1 \right] . \quad (10)$$

To compare the results from the hydraulic analogy with values for air a conversion to $\gamma = 1.4$ is necessary. The conversion below was previously used at Georgia Tech by Ryle¹² and is based on the work of Orlin, Linder and Bitterly⁸.

$$C_p = \frac{1}{M_s^2} \left[\left\{ \left(\frac{p}{p_0} \right)_{\gamma=1.4} \div \left(\frac{p}{p_0} \right)_{\gamma=2.0} \right\} \left(\frac{d}{d_s} \right)^2 - 1 \right] . \quad (11)$$

Thus by virtue of the hydraulic analogy applicable equations are set forth for the pressure coefficients from which airfoil characteristics data is obtained.

Transonic Flow over the Front Part of a Finite Wedge

General.--In subsonic flow the velocity will be zero at a sharp concave corner. Conversely, in subsonic flow at a sharp convex corner the theoretical velocity would approach infinity. But the upper limit of the subsonic range is finite so that a perfect fluid cannot flow about a

sharp convex corner without entering the supersonic range. From the zero value of velocity at the nose of the wedge the flow is accelerated to the sonic velocity at the shoulder. The fact that the entrance to a supersonic region requires a convex contour and the theoretical result that a sharp convex corner of a body necessarily makes the velocity exceed the subsonic range, lead to a most reliable fact about the flow around a wedge. The only possibility is that the sonic line starts at the shoulder (see Figure 3) and is followed by an expansion fan composed of an infinite series of Mach lines. The sonic line is at first perpendicular to the side of the wedge and is then bent around the corner.

The problem has been attacked in three parts: free-stream Mach number greater than one, equal to one, and less than one. These three parts of the problem are intimately related by the fact that the local Mach number distribution is independent of M_∞ when M_∞ is near unity. It is well known that the Mach number downstream of a weak, normal shock is as much below unity as the Mach number upstream is above unity. Thus there exists a certain symmetry about $M_\infty = 1$. For M_∞ very near unity the detached shock wave is far away from the wedge and is nearly normal; the Mach number just downstream of the shock is slightly subsonic. For the Mach number distribution on the wedge it is thus irrelevant whether this subsonic Mach at large distances is due to the presence of a shock wave or due to the fact that the velocity at infinity is slightly below sonic. Measurements by Griffith⁴ indicate that the Mach number distribution over the body is independent of the free-stream Mach number even for finite, small differences from $M_\infty = 1$. Mathematically, we have

$$\left(\frac{\partial M}{\partial M_\infty} \right)_{M_\infty=1} = 0 \quad (12)$$

where M is the local and M_∞ the free-stream Mach number.

Free-stream Mach number greater than one.---To handle the problem analytically, the flow must be determined in the transonic zone bounded by the bow wave, the wedge profile, and the separating Mach wave (see Figure 3a). The separating Mach wave is the particular expansion wave which meets the sonic line and the bow wave at their common point. Any disturbance introduced ahead of the separating wave can travel along a Mach wave to the sonic line and into the subsonic region, thereby influencing the shape of the boundaries.

The solution of the problem is complicated by the fact that the governing partial differential equation is of mixed type and non-linear.

$$\phi_{xx} \left(1 - \frac{u^2}{a^2} \right) + \phi_{yy} \left(1 - \frac{v^2}{a^2} \right) - 2\phi_{xy} \frac{uv}{a^2} = 0 \quad (13)$$

Moreover, the locations of the bow wave and the separating Mach wave are not known at the start but must be determined as part of the solution. The flow, having passed through the curved bow wave, is necessarily rotational which makes potential flow theory impossible to apply except as a perturbation. An additional practical complication arises from the fact that any rigorous solution must be a function of three independent variables, M_∞ , t/c , and δ .

Vincenti and Wagoner³ transformed the flow from the physical plane to the hodograph plane and introduced the assumption of small disturbances. Physically, this implies that the results are restricted to

thin airfoils at flight Mach numbers not far removed from unity. The transformation causes the bow wave to go over into a known shock polar, while the separating Mach wave transforms into one of the fixed epicycloids which make up the characteristic net in the hodograph. The terms representing fluid rotation turn out to be of the same order as other terms which are neglected in the analysis and they may be neglected. Now the differential equation, though still of the mixed type, takes on a specially simple form (the Tricomi equation) which has been the subject of considerable mathematical study.

$$\chi_{uu} = 2u, \chi_{vv} \quad (14)$$

where $u = a^* + u$, and ϕ is a function of χ , the transformed potential. Equation (14) is linear and can easily be solved by separation of variables. The solution of the problem becomes a function of a single parameter which involves all three of the individual variables previously discussed. This parameter is known as the transonic similarity parameter. It can be written in several forms, as, for example:

$$\xi_0 = \frac{M_s^2 - 1}{[(\gamma+1)(t/c)]^{2/3}} \quad (15)$$

Likewise, Karman¹³ showed that the perturbation equations hold for arbitrary values of t/c , γ , and M if

$$\xi_0 = \frac{M_s - 1}{[\frac{1}{2}(\gamma+1)(t/c)]^{2/3}}$$

is considered as the transonic similarity parameter. Karman's theory is

based on the existence of a potential flow, thus viscosity and rotation are neglected.

In the work of Vincenti and Wagoner³ the supersonic portion is replaced by an equivalent integral relation which must be satisfied everywhere along the sonic line. The differential equation becomes purely elliptic. By means of finite-difference approximations, the boundary value problem for the partial differential equation is reduced to a system of simultaneous algebraic equations. The latter problem is solved in normal fashion by relaxation techniques. Calculations have been carried out for sufficient values of ξ_0 to bridge the gap between the findings of Guderley and Yoshihara at $M_S = 1$ ($\xi_0 = 0$) and the analytical results which are available when the bow wave is attached and the flow is everywhere supersonic ($\xi_0 = 1.26$). These results are included in Figure 1 for the case of a 15° wedge in air.

Free-stream Mach number equal to one.--The formulation of the boundary value problem in the hodograph plane does not present great difficulty. Guderley and Yoshihara² introduce the quantity η by means of the relation

$$\eta = (\gamma + 1)^{1/3} \left(\frac{u - a^*}{a^*} \right)$$

and the differentiation equation for the transformed potential assumes the form

$$\phi_{\eta\eta} - \eta \phi_{\theta\theta} = 0 \quad (16)$$

which is Tricomi's equation. The singularity at the point of the hodograph which corresponds to the free-stream velocity has previously been investigated¹³. The transformation to the hodograph is order-reversing for lines of $y = \text{constant}$. A line representing y , for $y_1 < y_2$ will be affected more by the wedge, and its plot in the hodograph will be farther removed from the free-stream velocity than the line representing y_2 . From the behavior of y on the line $v = 0$, namely

$$y = 0 \quad u \neq a^* , \quad y = \infty \quad u = a^*$$

and from the behavior of the lines $y = \text{constant}$ near $u = a^*$ it can be inferred that locally y has a doublet singularity. A family of particular solutions suitable to fulfill the boundary conditions by superposition is easily found. However, a direct attempt to carry out this superposition leads to an infinite system of equations. Guderley and Yoshihara² found that an attempt to satisfy this system by taking a finite number of terms was too satisfactory. They showed how to overcome this difficulty. First, the boundary value problem is changed in such a way that the solution remains the same while the supersonic part of the boundary is more conveniently located. This change reduced considerably the amount of work required to establish the infinite system of equations. Then in the case of zero angle of attack the problem can be formulated in terms of an integral equation

$$-\frac{3}{2} \left(\frac{3}{4} \theta_0 \right)^{-1/3} \sum_{m=1}^{\infty} \int_0^{\theta_0/2} p(t) \sin \frac{m\pi t}{\theta_0} dt \cos \frac{m\pi(\theta_0 - \theta)}{\theta_0} = F_1(v) \quad (17)$$

where $0 \leq t \leq \theta_0/2$ and $0 \leq (\theta_0 - \theta) \leq \theta_0/2$, t is a variable of integration, and

$F_1(V)$ is a previously determined function. The kernel of equation (17) in a close approximation corresponds to that appearing in the theory of a thin airfoil in an incompressible flow. Thus the solution finally requires only a suitable Fourier analysis of the boundary conditions. The result for a 15° wedge in air is shown in Figure 1.

Free-stream Mach number less than one.--The problem of the wedge moving at Mach numbers slightly less than one has been solved by Cole¹. Steady, isentropic motion in a perfect, non-viscous gas is assumed; also, it is assumed that the flow field is perturbed about uniform flow at sonic velocity. If we let

$$U = - \frac{\delta + 1}{a^*} u,$$

$$V = \frac{\delta + 1}{a^*} v$$

the equations are

$$UU_x - V_y = 0 \quad (18)$$

$$U_y + V_x = 0 \quad (19)$$

When $U < 0$ the flow is supersonic and the system of equations (18) and (19) is hyperbolic. When $U > 0$ the flow is subsonic and the system is elliptic. Thus the system is of mixed type and is nonlinear.

In the hodograph plane the system of equations becomes linear and reduces to Tricomi's equation.

$$Uy_{vv} + Y_{uu} = 0 \quad (20)$$

With the boundary conditions of uniform flow at infinity (represented by a doublet singularity), flow tangent to the body, symmetry, sonic velocity at the beginning of the corner, and the stagnation condition of the linearized theory, and with the assumption that in turning the corner the flow is locally of the type investigated by Prandtl-Meyer, the equation can be solved mathematically.

However, other non-singular solutions will have to be added to the present one in order to satisfy the conditions in the supersonic region. These solutions, being non-singular, are likely to be of small magnitude. This solution is actually the solution to a problem where $x/c = 1$ on the sonic line. Replacing the sonic line by $x/c = 1$; should be a good approximation in the subsonic case, as far as the solution over the front part of the wedge is concerned.

For the linearized theory the pressure coefficient can be approximated as a linear function of the velocity and the drag coefficient can be found by integrating the pressure coefficient over the surface of the wedge.

$$C_p = -2 \frac{u - u_s}{u_s} \quad (21)$$

$$C_D = \theta_0 \int C_p d(x/c) \quad (22)$$

Cole's results for the case of a 15° wedge in air are included in Figure 1.

CHAPTER III

EQUIPMENT

There are two types of water channels suitable for application of the hydraulic analogy. The less expensive of these is the type in which the model is moved through static water. The other arrangement is one in which the model remains stationary while water flows past it. The former is in use at Georgia Tech and the Aerophysics Laboratory of North American Aviation, Incorporated⁹ while the latter is employed by the National Advisory Committee for Aeronautics at Langley Field, Virginia⁹.

Other advantages of the movable model type include easy acceleration of the flow, simple construction, and no boundary layer effect from the sides and bottom of the channel. Its biggest disadvantage, which is not present in the stationary model arrangement, is the difficulty of measuring the water depth along the model.

A general view of the water channel is shown in Figure 2. The frame is of bolted structural steel supporting a channel four feet wide, twenty feet long, and approximately one and one fourth inches in depth. The bottom of this channel is of plate glass in two five foot sections and one ten foot section. The transverse steel members are spaced at thirty inch intervals and are supported by screw jacks enabling the glass surface, over which the model slides, to be leveled within 0.001 inch in all points. This leveling is accomplished through the use of a transit.

A drain is provided at one end of the channel.

The model carriage is of welded steel tubing construction. It is moved along the channel on four rubber wheels which transfer the weight of the carriage to the upper horizontal steel member of the frame, serving also as rails. Four rubber wheels with vertical axes located at the carriage frame corners prevent any relative sidewise motion of the carriage. The model is supported behind the carriage by a vertically free acting mount producing the towing force and permitting the model weight to act on the channel bottom. This mount is also radially adjustable. Safety stops are placed at the ends of the carriage track to prevent overrunning of the carriage and model.

The carriage is driven by a one quarter horse-power, single phase, alternating current electric motor through a 3/32 inch continuous steel cable. A reversing mechanism and a "Speed-Ranger" device enable control of motion in either direction and at varied speeds. An auxiliary power unit is available for high speed and accelerating and decelerating runs. This consists of a 19.5 ampere, 24 volt direct current series wound motor which drives the cable through a set of reduction gears.

The combination of these two drive units provides speeds of from 0.5 to 5.5 feet per second.

The correct timing for accurate speed adjustment of the model is accomplished by means of a microswitch placed on the track. A cam 2.925 feet in length attached to the carriage trips this switch which automatically operates an electric timer. The timer is located on the control panel at the side of the water channel. This panel also contains the instruments and switches for starting, reversing and operating the drive mechanism.

When experimental work was first begun in the Georgia Tech water channel, photographs were taken of the models to determine the water depth distribution around the model. The method and equipment used in this work are described by Hatch¹⁵. Photographic interpretation of these results was not particularly accurate so another method of measuring water depth was developed.

The model is fitted with a plexiglas bracket from which are suspended steel needle probes alongside the model. These probes are attached to adjustable brass screws, which are mounted in the plexiglas bracket. Copper contacts are provided for each probe. Contact of the probe with the water completes the grid circuit of a vacuum tube causing a relay to operate a signal light. As the model is moved through the water, the probe is adjusted vertically until it just touches the water. The status of the signal light determines the contact position of the probe point and the water surface. This is done for each of the probes and the probe heights from the bottom of the model are then measured by means of a height gage and surface plate to within an accuracy of 0.001 inch.

The model was chosen because of the availability of shock tube data. The model is a wedge airfoil and is constructed of aluminum. A descriptive diagram is shown in Figure 4.

CHAPTER IV

PROCEDURE

Preliminary runs were made for the purpose of aligning the model. The model was set at zero angle of attack by measuring the water depth at similar points on each side of the model and adjusting the model until the two readings were identical.

The meniscus effect of the water was measured and recorded for use in correcting the water depths to the actual values caused by the hydraulic analogy. These measurements were made with the model stationary.

The water depth was set before each run by means of a probe which was adjusted to 0.250 inch. The model speed was regulated to the desired value by the use of the electric timer. The probes were then adjusted until they indicated the local depths of the water alongside the model; they were left slightly out of the water to prevent interference with the flow pattern. The probe heights were measured and recorded for use in calculating the pressure coefficients. Tests were conducted at Mach numbers of 0.852, 0.97, 1.08, and 1.20.

CHAPTER V

DISCUSSION OF RESULTS

The meniscus effect on the side of the model as measured with the model stationary is shown in Figure 5. Since the effect close to the side of the model is of the order of 0.020 to 0.040 inch, it is clearly not a negligible quantity.

The calculated pressure coefficients, shown in Figure 6, do not have the same shape as predicted by the theory² and verified by shock tube experiments⁴. The theoretical curves have an appreciable slope whereas the water channel results indicate an almost constant pressure coefficient from about $x/c = 0.2$ to $x/c = 0.8$.

It is felt that the pressure coefficient curve does not have the predicted shape, because of the effect of vertical accelerations in the water channel. In the theory of the hydraulic analogy, vertical accelerations are neglected. If the water channel were to follow the predictions of the theory, the water depth at the nose of the wedge should reach the stagnation value at speeds below the speed at which the bow wave attaches to the nose. Consider the equation for the stagnation depth¹⁶.

$$d_0 = d_s \left[1 + \frac{M_s^2}{2} \right]$$

For $M_s = 0.8$, $d_0 = 1.32d_s$ and for a static water depth of 0.25 inch the increase to stagnation value is only 0.08 inch. This increase can be almost fully realized without a large vertical acceleration. But for

$M_S = 1.2$, $d_0 = 1.72 d_S$, and for a static depth of 0.25 inch the difference in static and stagnation depth is 0.18 inch. An appreciable vertical acceleration is required for the depth to increase by almost three-fourths of its original depth. The results of Laitone and Nielsen¹⁷ obtained by hydraulic analogy also show a depth at the nose of the wedge which is appreciably less than the stagnation depth in the transonic range of velocities.

From Figure 6 it is obvious that of the four pressure coefficient distributions the one at the lowest Mach number (0.852) most nearly approaches the theoretical shape in that it shows an appreciable pressure rise at the nose of the airfoil.

Except for $M = 0.97$ the values of C_p on the rear portion of the airfoil agree well with the theory and the experimental results in air¹⁸. For $M = 0.97$ it appears that the channel is not long enough to allow steady state to be reached; i.e., for the bow wave which is formed in starting the model to disappear upstream, and therefore the pressures measured are slightly larger than they should be.

The drag coefficients obtained by integrating the pressure coefficient times the tangent of the semi-wedge angle along the chord are shown in Figure 1. The value for $M_S = 0.852$ is within the experimental accuracy at this condition. The experimental accuracy is not too good because, as discussed below, the depth ratios are near unity. The value for $M_S = 0.97$ is high because it is believed that steady state was not reached. The values for $M_S = 1.08$ and 1.20 are low because the effect of the vertical accelerations prevents the proper pressure increase at the nose of the wedge.

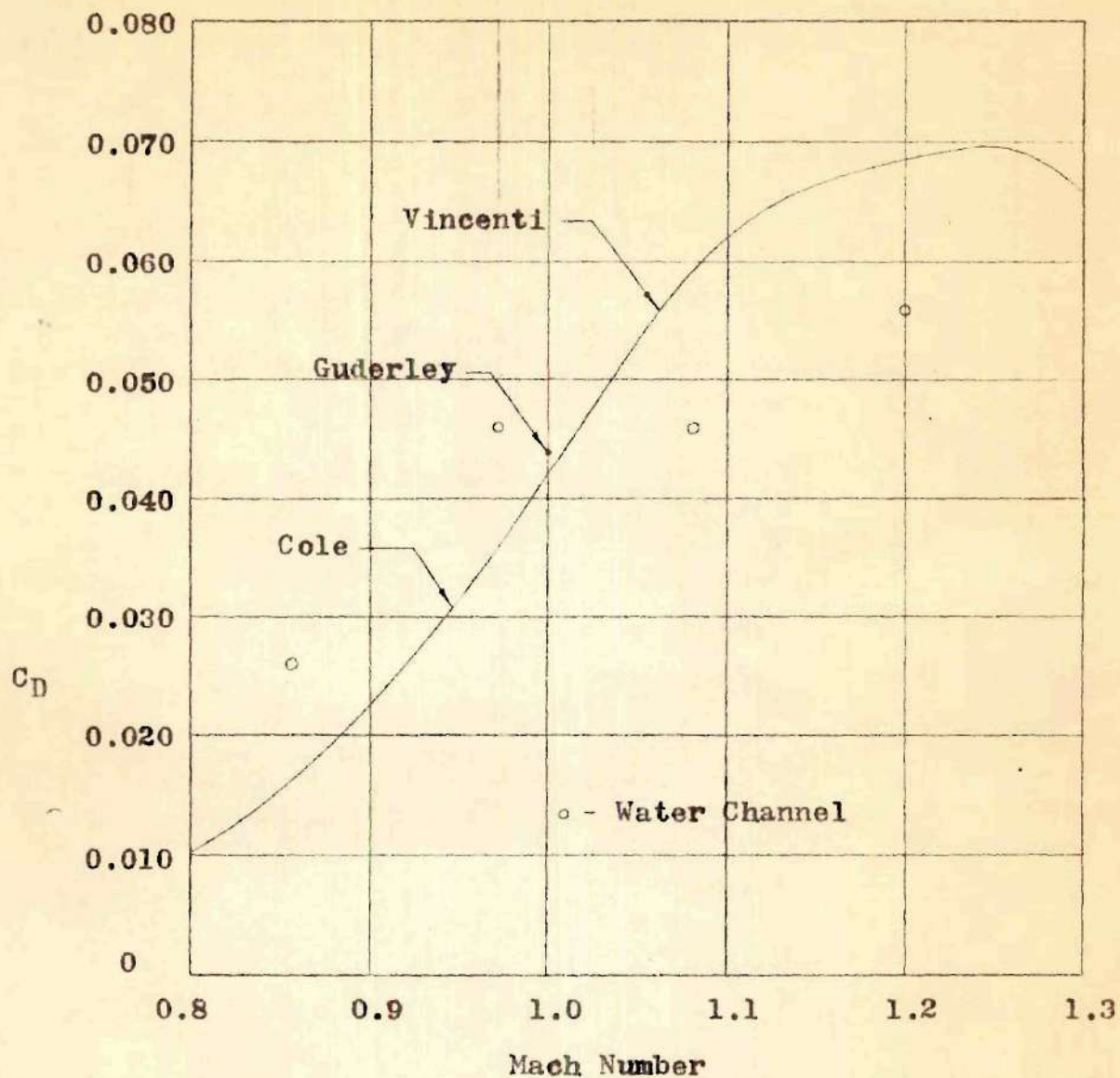


Figure 1--Pressure Drag Coefficient for a 15° Wedge
at Zero Angle of Attack

The values of the pressure coefficient, and therefore the drag coefficient, are subject to error because of the nature of the equation used to calculate C_p .

$$C_p = \frac{1}{M_s^2} \left[\left\{ \left(\frac{p}{p_0} \right)_{\gamma=1.4} \div \left(\frac{p}{p_0} \right)_{\gamma=2.0} \right\} \left(\frac{d}{d_s} \right)^2 - 1 \right] \quad (11)$$

A small error in d/d_s , particularly for values close to unity, will cause a considerable error in C_p . The γ correction is possibly a source of small error, but the error should not be great since it depends on values taken from Figure 1 of the National Advisory Committee for Aeronautics Technical Note 1185.⁸

CHAPTER VI

CONCLUSIONS

1. The effect of the meniscus along the side of the model is sizable, and must be taken into account when evaluating water channel test data.
2. For investigations at Froude (Mach) numbers slightly below 1.0, the moving model and static water arrangement does not allow steady state to be reached in a short run and does not give reliable results.
3. For Mach numbers greater than approximately 0.8 the hydraulic analogy does not give accurate results in the vicinity of a stagnation point.
4. The drag coefficients obtained in the transonic range by this investigation do not provide a valid, accurate comparison with the theory.

CHAPTER VII

RECOMMENDATIONS

1. A more accurate method of adjusting the probe to the water level than that used at present at Georgia Tech would provide greater experimental accuracy for the water channel.

2. A more complete and accurate investigation of the meniscus effect would add to the usefulness of the water channel as a research tool.

APPENDIX

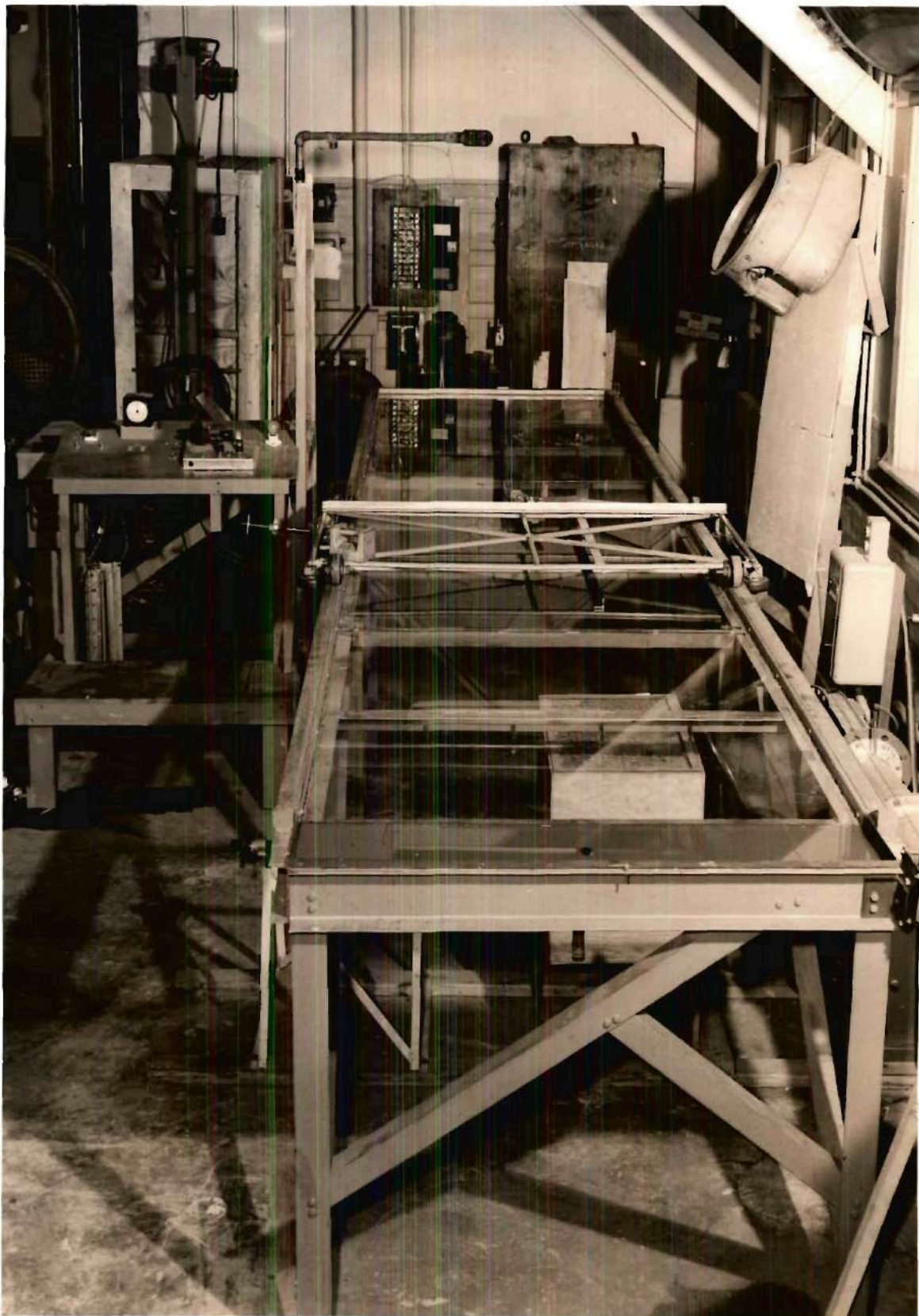


Figure 2. General View of the Water Channel

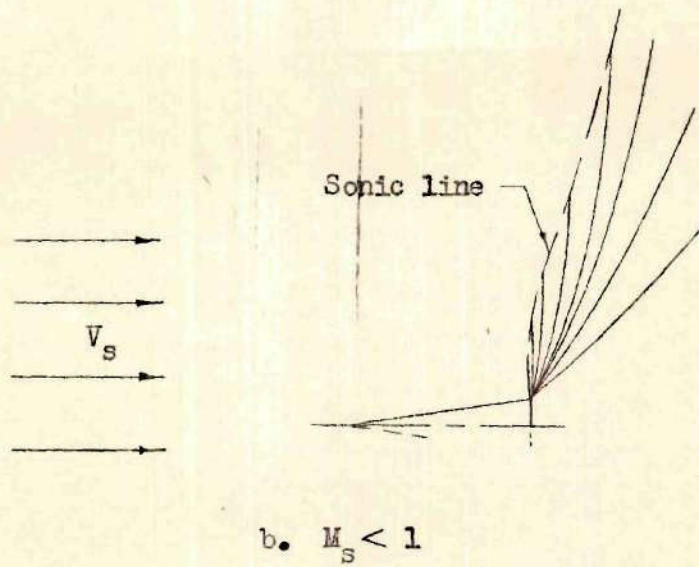
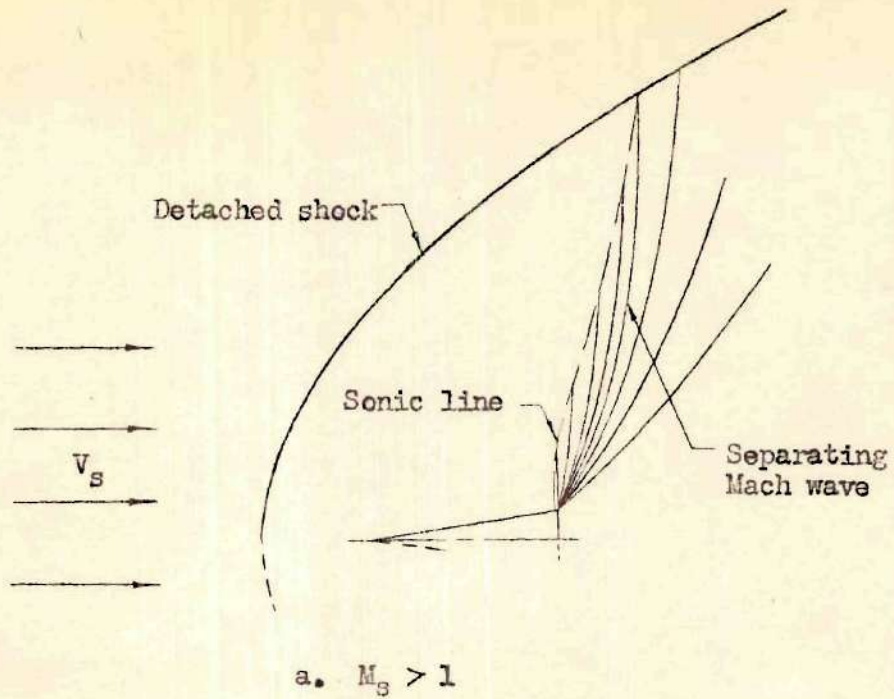


Figure 3. Transonic Flow Around a Wedge Airfoil

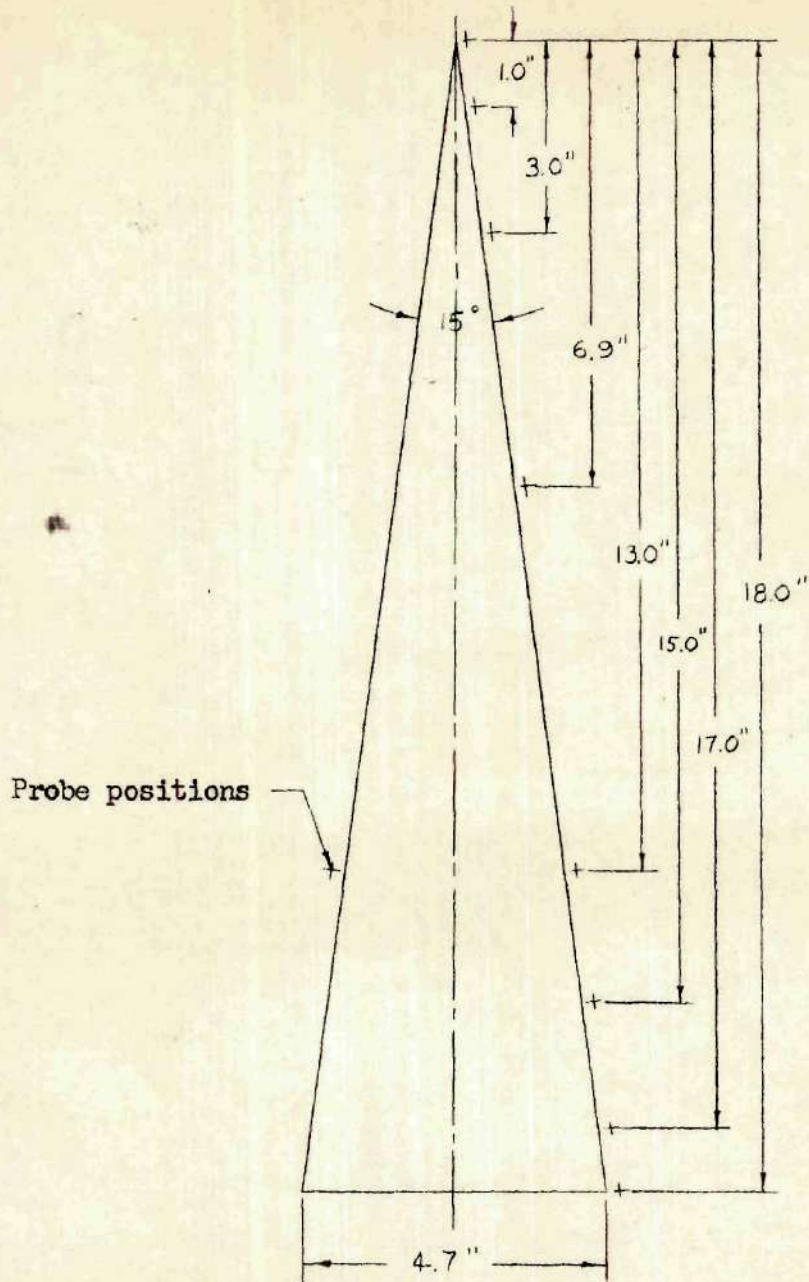


Figure 4. Wedge Airfoil Model

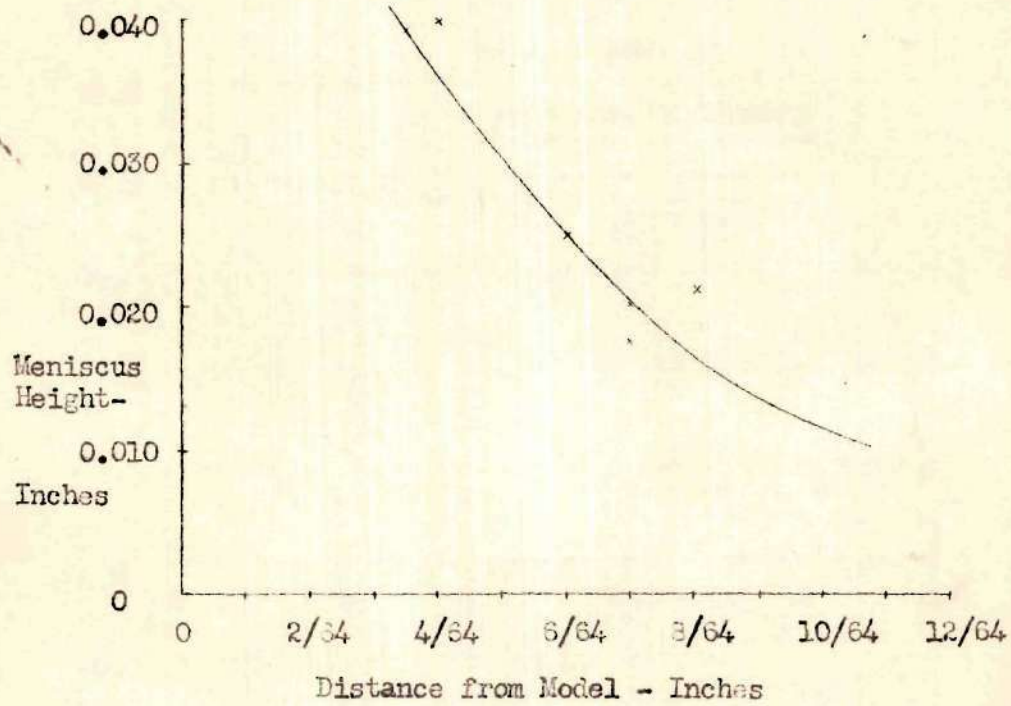


Figure 5. Meniscus Effect

BIBLIOGRAPHY

1. Cole, Julian D., "Drag of a Finite Wedge at High Subsonic Speeds," Journal of Mathematics and Physics, 30, 79-93, (1951)
2. Guderley, G., and Yoshihara, H., "The Flow over a Wedge Profile at Mach Number 1," Journal of the Aeronautical Sciences, 17, 723-735 (1950)
3. Vincenti, Walter D., and Wagoner, Cleo B., "Transonic Flow Past a Wedge Profile with Detached Bow Wave - General Analytical Method and Calculated Results" National Advisory Committee for Aeronautics Technical Note 2339, (1951)
4. Griffith, Wayland, "Shock-Tube Studies of Transonic Flow over Wedge Profiles," Journal of the Aeronautical Sciences, 19, 249-257, (1952)
5. Riabouchinsky, D., "Mecanique des Fluides," Comptes Rendus, 195, 998-999, (1932)
6. Preiswerk, Ernst, "Application of the Methods of Gas Dynamics to Water Flows with Free Surface."
Part I. "Flows with no Energy Dissipation," National Advisory Committee for Aeronautics Technical Memorandum 934, (1940)
Part II. "Flows with Momentum Discontinuities (Hydraulic Jumps)," National Advisory Committee for Aeronautics Technical Memorandum 935, (1940)
7. Binnie, A. M. and Hooker, S. G., "The Flow under Gravity of an Incompressible and Inviscid Fluid through a Constriction in a Horizontal Channel," Proceedings of the Royal Society of London, 159A, 592-608, (1937)
8. Orlin, W. James; Linder, Norman J.,; and Bitterly, Jack G., "Application of the Analogy Between Water Flow with a Free Surface and Two-Dimensional Compressible Gas Flow", National Advisory Committee for Aeronautics Technical Note 1185, (1947)
9. Bruman, J. R., "Application of the Water Channel Compressible Gas Analogy," North American Aviation Incorporated Engineering Report NA-47-87, (1947)
10. Crossley, H. E., Jr.; Harleman, D. R. F.; and Ippen, A. T, "Studies on the Validity of the Hydraulic Analogy to Supersonic Flow," United States Air Force Technical Report 5985, (1950-1952)

11. Page, Leigh, Introduction to Theoretical Physics, 218-234, D. Van Nostrand Co., Inc., (1928)
12. Ryle, Dallas Marlin, Jr., "Application of the Hydraulic Analogy to Study the Performance of Three Airfoils at Subsonic and Supersonic Speeds," Unpublished Masters Thesis, Georgia Institute of Technology, (1950)
13. Van Karman, Theodore, "The Similarity Law of Transonic Flow", Journal of Mathematics and Physics, 26, 182-190, (1947)
14. Guderley, Gottfried, "Singularities at the Sonic Velocity," United States Air Force Report F-TR-1171-ND, (1948)
15. Hatch, John Elmer, Jr., "The Application of the Hydraulic Analogy to Problems of Two-Dimensional Compressible Gas Flow," Unpublished Masters Thesis, Georgia Institute of Technology, (1949)
16. Orlin, Linder, and Bitterley, Op. Cit., p. 7
17. Laitone, E. V., and Nielsen, H., "Transonic Flow past Wedge Profiles by Hydraulic Analogy", Journal of the Aeronautical Sciences, 21, 498, (1954)
18. Griffith, Op. Cit., Fig. 15, p. 257

